Investigation of GaAs and AlAs Atomic Layer Epitaxial Growth Mechanism Based on Experimental Results and First-principles Total Energy Calculation

Nobuyuki Ohtsuka[1], Masato Oda[1], Takashi Eshita[1,2], Ichiro Tanaka[1] , and Chihiro Itoh[1]

[1] *Faculty of Systems Engineering, Wakayama University, Wakayama 640-8510, Japan*
[2] *Fujitsu Semiconductor Limited, Yokohama 222-0033, Japan*

E-mail: s179002@wakayama-u.au.jp

In the GaAs and AlAs atomic-layer epitaxy (ALE), it has been experimentally found that AlAs layer is deposited by two mono layers (2 ML) per one ALE cycle while GaAs layer is deposited by one mono layer (1 ML). In order to elucidate this growth mechanism, we compare the stability of Ga and Al atoms on the GaAs (100) surface by the first-principles total energy calculation based on the density functional theory (DFT). Comparing adsorption energies, we find that Ga and Al stably absorbed on the As-terminated GaAs surface in 1 ML. It is also revealed that Al can adsorb on As-terminated GaAs (100) surface with the amount of 2 ML because excess Al atoms can be adsorbed by forming a metallic Al (110) plane like structure. Those results well explain experimental results for ALE-GaAs and ALE-AlAs.

1. Introduction

In the recent evolution of Artificial Intelligence (AI) and Internet of Things (IoT) used in our various fields, semiconductor devices are playing an important role as their indispensable and fundamental technology.[1-4] Although current semiconductor devices fabricated by the technology node with less than 10 nm, the future IoT and AI will demand the semiconductor devices to have much higher performance, such as high speed and low power consumption. Thus, the future semiconductor devices should be fabricated by using the more shrunk technology nodes. However, it has been reported that those semiconductor devices are difficult to fabricate along with the Moore's law, which predicts that the number of transistors in an integrated circuit doubles about every two years, because of their physical limitations .[5] Therefore, the break-through technologies so-called by the "More than Moore" for those semiconductor devices are necessary to sustain the evolution of AI and IoT. [6] Semiconductor thin film deposition technique is one of the most crucial technologies for the More than Moore's technology. Atomic layer epitaxy (ALE) is the most promising candidate because of its atomically controlled layer by layer deposition due to the self-limiting mechanism. [7-19]

In the fabrication of atomic layer epitaxial GaAs (ALE-GaAs) using trimethylgallium (TMG) as a Ga source gas, it has been experimentally found that GaAs layer is deposited with one mono layer (1 ML) per one ALE cycle by the self-limiting mechanism. [11] In the case of ALE-AlAs using trimethylaluminum (TMA) as an Al source gas, it has been reported that the self-limiting mechanism worked in 2 ML and 3 ML.[20] Furthermore, self-limiting growth at either 1 ML or 2 ML per ALE cycle is clearly observed using ethyldimethylamine alane (EDMAAl) and arsine (AsH_3) as Al and As sources and trimethylaminne-alane (TMAAl) and tris–dimethylamino-arsinic $\{As[N(CH_3)_2]_3\}$ as Al and As sources.[21, 22]

The self-limiting mechanism for 1 ML ALE-GaAs has been explained by the selective adsorption model[11] or the adsorbed-source-gas inhibition model.[8] We have proposed a selective adsorption model that TMG is decomposed on the GaAs surface to form a Ga 1 ML and extra adsorbed TMG is desorbed without decomposition, which was obtained by in-situ X-ray photoelectron spectroscopy (XPS) observation.[23] In ALE-AlAs, the self-limiting seems to work in 2 ML rather than 1 ML.[20] **It was** reported that Al is adsorbed with 2 ML as a metal structure on the GaAs surface which is obtained by experimental results and the calculation result using tight-binding method.[20, 24, 25] Fujii observed that 2 ML Al self-limiting growth occurred following 1 ML Al self-limiting growth at growth temperature of 350 ℃ **by** the measurement of quadrupole mass spectrometric (QMS) and temperature programmed desorption (TDS).[22] However, their growth models are not necessarily clear because their results were derived from empirical calculations using experimental results. In addition, there are few reports comparing the reason why the self-limiting mechanism works in 2 ML of ALE-AlAs and the self-limiting mechanism does not work in 2 ML of ALE-GaAs.

In this paper, we compare the stability of Ga and Al atoms on the As-terminated GaAs surface using first-principles total energy calculations. As the calculation results, it is revealed that Al atoms can be deposited with the amount of 2 ML on the As-terminated GaAs substrate, although 1 ML deposition is slightly more stable. On the other hand, Ga atoms cannot be deposited with the amount of 2 ML. In this study, we refine the discussion on the difference for the growth mechanism of ALE-Ga and ALE-Al in addition to our already reported study. [26]

2. Experimental methods

2.1 ALE Gas pulse sequence and apparatus configuration

We used TMA, TMG, and AsH_3 for source gases of Al, Ga and As, respectively, with H_2 carrier gas. Figure 1 shows the source-gas supplying sequence for ALE-GaAs and ALE-AlAs. The source-gas of TMA or TMG and AsH_3 were separately supply to the growth chamber. Before supplying each source gas, growth chamber was purged by H_2 gas. The gas pulse duration of AsH_3 and H_2-carrier gas were 10 s and 3 s, respectively. One ALE cycle is defined as shown in Fig. 1.

ALE growth was carried out in the growth chamber, as shown in Fig. 2, at 500 ℃. The total gas flow rate was 2 SLM and the growth pressure was kept at 20 Torr.[27] The mole fractions for TMA, TMG and AsH_3 were 1.0×10^{-3}, 1.0×10^{-3} and 2.4×10^{-2}, respectively. We measured the film thickness by measuring the step height after partially removing the growth film with stripe pattern. The deposition comparison between ALE-AlAs and ALE-GaAs was done with these similar growth conditions and deposition device.[11, 20]

2.2 Computational method

To evaluate the adsorption energies of the system, we used the PHASE code[28, 29], program package for performing first-principles total energy calculations based on density functional theory (DFT)[30] and the ultra-soft pseudo-potential scheme. The generalized gradient approximation was used as the exchange-correlation term.[31] The cutoff energies for the wave function and charge density were 30 and 120 Ry, respectively. A 5 layered GaAs (100) 4 x 4 surface was employed for the basic substrates as shown in Fig. 3. The back surface was terminated with pseudo hydrogen atoms that have +075*e*. The lattice constant of the model was 5.702Å in this study, which is well reproducing the previously reported experimental value.[32] The Brillion zone integration was performed using a 4 x 4 x 1 mesh.

We define the adsorption energy (E_{ad}) :

$$E_{\mathrm{ad}} = (E_{\mathrm{total}} - E_{\mathrm{sub}})/N - E_{\mathrm{atom}} \qquad (1)$$

Where E_{total}, E_{sub}, E_{atom}, and N are total energy of the system, total energy of the substrate, total energy of a single adsorbed atom, and number of adsorbed atoms, respectively.[33)]

To calculate E_{ad}, we put the adsorbate atoms as the ideal epitaxial position for 1 ML model and from ideal (110) plane of fcc crystals for 2 ML model, respectively as shown in Fig. 3. We selected the ideal (110) plane of the fcc crystal as 2ML model because it was reported that 2ML Al atoms existed as a fcc crystal on the GaAs surface [ref.]（2 MLモデルの場合はfcc結晶の理想的な（110）面選んだのは、GaAs表面上に2 MLのAl原子がのfcc結晶として存在することが報告されているからである。）Although there is no report on 2ML Ga atoms on the GaAs (100) surface, we selected the same structure as Al atoms for comparison with the Ga atoms on GaAs in this study.（GaAs（100）表面上の2MLのGa原子に関しての報告は見当たらないが、今回の検討においては比較のためにAl原子と同様な構造を用いることとした。）In the case of the 2ML model, the ideal (110) plane of the fcc crystal was selected because it was reported that 2ML Al atoms existed as a fcc crystal on the GaAs surface.Then, we optimized the atomic positions of upper 3-layers by reducing the maximum force on each atom to less than 10^{-3} Ht/bohr. It is well known that a cleaned As- terminated surface of the GaAs (100) is often reconstructed into a dimer structure. In the ALE growth process, we consider that the dimerized As should open and relax to the ideal site when Ga atoms are introduced into As-terminated surface, resulting in the formation of normal As-Ga bond. In this study, we used the above mentioned ideal site model instead of the dimer structure model to make clear the differences between the

two cases of the self-limiting mechanism works with 1 ML and works with 2 ML. It is noted that we employed the ideal (110) plane for 2 ML models because the growth rate of our ALD process is very low of approximately 75 nm / h at 500℃.[34, 35] It has been reported that the stable adsorption site changes depending on the Ga coverage on the GaAs (100) surface.[36] (

GaAs (100)表面上のGaの被覆率に応じて安定した吸着サイトが変化することが報告されています) However, in this paper, in order to make a comparative study based on the experimental results after the supply of source-gases was completed, the stable adsorption site was assumed to be constant without taking into account the intermediate Ga coverage.(しかし、この論文においては、原料供給の終了した実験結果を基に比較検討を行うために、途中経過となるGaの被覆率は考慮せず安定吸着サイトは一定であるものといたしました。)Since Sakuma[37] reported that the film thickness does not change even if the purge time after stopping the TMG supply is increased during ALE process at 500 ℃, it is also considered that adsorption and desorption on the outermost surface of the GaAs should not occur in our ALD process.

3. Results and discussion

Figure 4 shows relationship between the growth rate and the pulse duration of source gases of TMG and TMA. It is noted that ALE-GaAs and ALE-AlAs were deposited respectively, and we summarize the results in Fig. 4 for the sake of comparison.[11, 20] These results clearly show the self-limiting growth behavior of 1 ML for GaAs and 2 ML for AlAs, respectively.

Figure 5 (a) and (b) show optimized structures of Ga atoms on the As-terminated GaAs (100) surface with 1 ML and 2 ML structure, respectively. And also Fig. 6 (a) and (b) show

optimized structures of Al atoms on the As-terminated GaAs (100) surface with 1 ML and 2 ML structure, respectively. As explained in the previous section, the atomic position for the relaxation is starting from the ideal GaAs(100) surface. These results show that surface structures represent at least a kind of local minimum structures. Both 2 ML models exhibit little bit bumpy structure to release the steric repulsion. In the case of Ga, we obtained the adsorption energy of -3.34 eV for 1 ML adsorption, and -3.13 eV for 2 ML adsorption. These results indicate that 1 ML Ga more stably adsorbed on As-terminated GaAs (100) than 2 ML Ga, which corresponds to the experimental result as shown in Fig. 4. In the case of Al, we obtained the adsorption energy of -3.78 eV for 1 ML and -3.72 eV for 2 ML. 1 ML adsorption is also more stable than 2 ML absorption for Al. However, the adsorption energy difference of 0.06 eV between 1 ML-Al and 2 ML-Al is much smaller than that of 0.21 eV between 1 ML-Ga and 2 ML-Ga. Thermal energy of the growth temperature of 500 ℃ is about 0.07 eV which is slightly higher than the adsorption energy difference 1 ML and 2 ML for Al of 0.06 eV. In the case of ALE-AlAs, it is considered that when excess Al atoms are supplied at the growth temperature of 500 ℃, the 2 ML Al is realized beyond the 0.06 eV barrier. This should be the reason why the self-limiting mechanism in 1 ML Al does not work at 500 ℃. Fujii[22] reported that 2 ML Al self-limiting growth was observed following by 1 ML Al self-limiting growth at 350 ° C in ALE-AlAs. In their report, self-limiting growth of 1 ML and 2 ML clearly appears. We can explain their Al growth behavior consistently with our adsorption energy model. First, only 1 ML Al structure is realized with low growth temperature of 350 ℃, corresponding to the thermal energy of 0.05 eV which is slightly smaller than the adsorption energy difference between the 1 ML and 2 ML Al, thus resulting in slow generation of 2 ML-Al. In addition, because the energy difference of 0.21 eV

between 1 ML-Ga and 2 ML- Ga is higher than the thermal energy of 0.07 eV at the growth temperature of 500 ℃, it should be difficult for Ga to adsorb on GaAs with 2 ML.

From these results, we propose the growth mechanism for ALE-GaAs and ALE-AlAs. Figure 7 shows the growth model for the ALE-GaAs. We assume the initial surface before the Ga desorption is As-terminated GaAs (100) 4x4 surface. When TMG is supplied into the growth chamber, Ga atoms generated from decomposed TMG are adsorbed on the As-terminated GaAs (100) surface and stabilized with 1 ML structure. Further Ga-atom adsorption and construction of 2 ML does not occur because adsorption energy generating 2 ML requires much higher energy than 0.21 eV. And then, when AsH_3 is supplied to the growth chamber, 1 ML GaAs is formed by reaction of 1 ML-adsorbed Ga and in As from AsH_3.

Figure 8 shows the growth model for ALE-AlAs. The initial surface before the ALE growth is assumed to be As-terminated GaAs (100) 4x4 surface. When TMA is supplied into the growth chamber, Al atoms generated from decomposed TMA are adsorbed on the As-terminated GaAs (100) surface and stabilized with 1 ML structure. Because the difference of adsorption energy of Al between the 2 ML and 1 ML is 0.06 eV, further adsorption occurs and 2 ML Al Atoms are stabilized. And, when AsH_3 is supplied to the growth chamber, 2 ML AlAs is formed by reaction of 2 ML adsorbed Al and As from AsH_3.

4. Conclusions

We compared the adsorption energy of Ga and Al atoms on As-terminated GaAs (100) surface using first-principles total energy calculations. It is revealed that 1 ML adsorption is stable both for Ga and Al atoms. Adsorption energy differences of 1 ML and 2 ML of Ga

and Al are 0.21 eV and 0.06 eV, respectively. Since the thermal energy of growth temperature of 500 ℃ is about 0.07 eV, 1 ML Al self-limiting mechanism does not work and the amount of 2 ML Al easily adsorbs on the GaAs surface by excessively supplied Al. On the other hand, Ga atoms tend to adsorb on As-terminated GaAs (100) surface with 1 ML structure because of high adsorption energy difference of 0.21 eV between 1 ML Ga and 2 ML Ga. Those results well explain experimental results for ALE-GaAs and ALE-AlAs.

Acknowledgments

The authors would like to thank Mr. Yasunori Yoshijima in Fujitsu Semiconductor for continuous encouragement for this work. The present study was partially supported by JSPS KAKENHI grant Nos. JP17H05339 and JP19H04547.

References

1) Y. Matveyev, K. Egorov, A. Markeev, and A. Zenkevich, J. Appl. Phy. **117,** 044901 (2015).

2) S. K. Vishwanath, H. Woo, and S. Jeon, Nanotechnology. **29,** 235202 (2018).

3) Y. Morita, K. Fukuda, Y. Liu, T. Mori, W. Mizubayashi, S. O'uchi, H. Fuketa, S. Otsuka, S. Migita, M. Masahara, K. Endo, H. Ota, and T. Matsukawa, Jpn. J. Appl. Phys. **56,** 04CD19 (2017).

4) T. Eshita, W. Wang, K. Nomura, K. Nakamura, H. Saito, H. Yamaguchi, S. Mihara, Y. Hikosaka, Y. Kataoka, and M. Kojima, Jpn. J. Appl. Phys.**57**, 11UA01 (2018).

5) C. A. Mack, IEEE Transactions on SEMI. Manufacturing. **24,** 202 (2011).

6) M. M. Waldrop, Nature. **530,** 144 (2016).

7) T Suntola, and J. Antson, U.S. Pat 4058430 (1977)

8) J. Nishizawa, H. Abe, and T. Kurabayashi, J. Electrochem. Sci. **132,** 1157 (1985).

9) A. Usui, and H. Sunakawa, Jpn. J. Appl. Phys. **25,** 212 (1986).

10) A. Doi, Y. Aoyagi, and S. Namba, Appl. Phys. Lett. **49,** 785 (1986).

11) M. Ozeki, K. Mochizuki, N. Ohtsuka, and K. Kodama, Appl. Phys. Lett. **53,** 1509 (1988).

12) Y. Sakuma, K. Kodama, and M. Ozeki, Appl. Phys. Lett. **56,** 827 (1990).

13) N. Ohtsuka, K. Kitahara, M. Ozeki, and K. Kodama, J. Crystal Growth **99,** 346 (1990).

14) K. Mukai, N. Ohtsuka, and M. Sugawara, Appl. Phys. Lett. **70,** 2416 (1997).

15) A. Furuya, K, Yoneda, E. Soda, T. Yoshie, H. Okamura, M. Shimada, N. Ohtsuka, and S. Ogawa, J. Vac. Sci. Technol. B **23,** 2522 (2005).

16) T. Kurabayashi, e-J. Surf. Sci. Nanotech. **13,** 357 (2015).

17) H. Zhou, X. Lou, N. J. Conrad, M. Si, H. Wu, S. Alghamdi, S. Guo, R. G. Gordon, and P. D. Ye, IEEE ELECTRON DEVICE LET. **37,** 556 (2016).

18) F. Dvorak, R. Zazpe, M. Krbal, H. Sopha, J. Prikryl, S. Ng, L. Hromadko, F. Bures, and J. M. Macak, Appl. Materials Today **14,** 1 (2019).

19) B. T. Lin, W. H. Lee, J. Shieh, and M. J. Chen, Proc. of SPIE. **10968,** 1096816 (2019).

20) M. Ozeki, and N. Ohtsuka, Appl. Surf. Sci. **82/84,** 233 (1994).

21) S. Hirose, M. Yamaura, A. Yoshida, H. Ibuka, K. Hara, and H. Munekata, J. Crystal Growth **194,** 16 (1998).

22) K. Fujii, I. Suemune, and M. Yamanishi, Appl. Phys. Lett. **62,** 1420 (1993).

23) K. Kodama, M. Ozeki, K. Mochizuki, and N. Ohtsuka, Appl. Phys. Lett. **54,** 656 (1989).

24) K. Kitahara, N. Ohtsuka, and M. Ozeki, J. Vac. Sci. Technol. B **7,** 700 (1989).

25) J. C. Duran, G. Platero, and F. Flores, Phys. Rev. B **34,** 2389 (1986).

26) N. Ohtsuka, M. Oda, T. Eshita, I. Tanaka, and C. Itoh, Ext. Abstr. 2019 Int. Conf. Solid State Devices and Materials, 2019, p. 283

27) M. Ozeki, N. Ohtsuka, Y. Sakuma, and K. Kodama, J. Crystal Growth **107,** 102 (1991).

28) National Institute of Materials Science, The PHASE Project [https://azuma.nims.go.jp/]

29) T. Yamasaki, A. Kuroda, T. Kato, J. Nara, J. Koga, T. Uda, K. Minami, and T. Ohno, Comput. Phys. Commun. **244,** 264 (2019).

30) P. Hohenberg and W. Kohn, Phys. Rev. **136**, B864 (1964).

31) J. P. Perdew, K. Bruke, and M. Ernzerhof, Phys. Rev. Lett. **77,** 3865 (1996).

32) A. Janotti, Su-Huai Wei, and S. B. Zhang, Phys. Rev. B **65**, 115203 (2002).

33) D. S. Sholl and J. A. Steckel, "DENSITY FUNCTIONAL THEORY, A Practical Introduction" (Johon Wiley & Sons, New Jersey, 2009), Chap. 4

34) P. M. Petroff, L. C. Feldman, A. Y. Cho, and R. S. Williams, J. Appl. Phys. **52**, 7317 (1981).

35) J. Massies, and N. T. Linh, Surf. Sci. **114**, 147 (1982).

36) T. Ito, K. Shiraishi, and T.Ohno, Appl. Surf. Sci. **82/84,** 208 (1994).

37) Y. Sakuma, Shunichi Muto, Kazuo Nakajima, and Naoki Yokoyama, Appl. Surf. Sci. **82/84,** 239 (1994).

Figure Captions

Fig. 1. Source gas supplying sequence for ALE-GaAs and ALE-AlAs. The vertical axis represents the source gas supply concentration, and the horizontal axis represents the source gas supply time. One ALE cycle is defined as TMG or TMA supply, H_2 purge , AsH_3 supply , H_2 purge.

Fig. 2. Schematic diagram of the growth system for ALE. The chimney type reactor with graphite susceptor setting the substrate is heated by the radio-frequency (RF) heating method. Source gases were abruptly exchanged using a pressure-balanced vent-and-run gas manifold.

Fig. 3. Schematic models for as-terminated GaAs (100) 4x4 surface supercell for a basic model for the calculation. Blue atoms show Ga atoms or Al atoms as the ideal epitaxial position for 1 ML model and from the ideal (110) plane of fcc crystals for 2 ML model.

Fig. 4. Growth rate dependence of ALE-GaAs and ALE-AlAs as a function of TMG and TMA pulse duration at 500 ℃.

Fig. 5. Schematic models from calculation results of adsorption energy for Ga 1 ML (a)

and 2 ML (b) on As-terminated GaAs (100) surface.

Fig. 6. Schematic models from calculation results of adsorption energy for Al 1 ML (a) and 2 ML (b) on As-terminated GaAs (100) surface.

Fig. 7. Growth model for ALE-GaAs. R shows the methyl radical.

Fig.8. Growth model for ALE-AlAs. R shows the methyl radical.

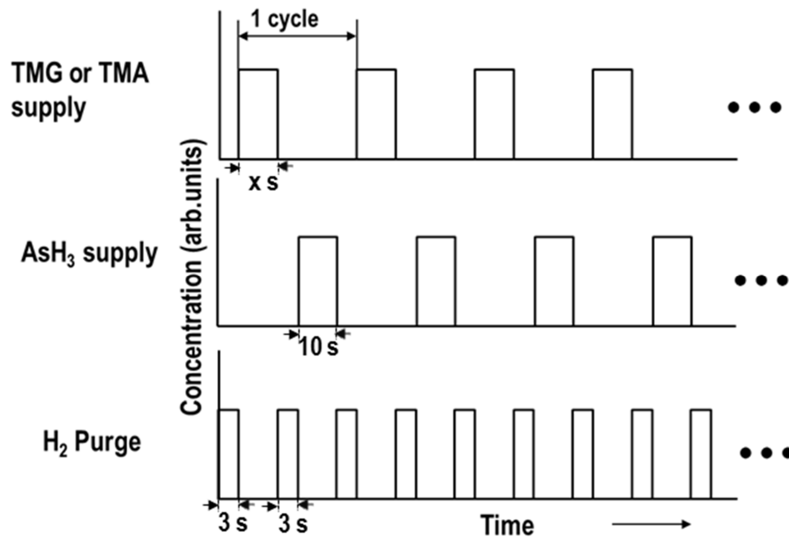

Fig.1.

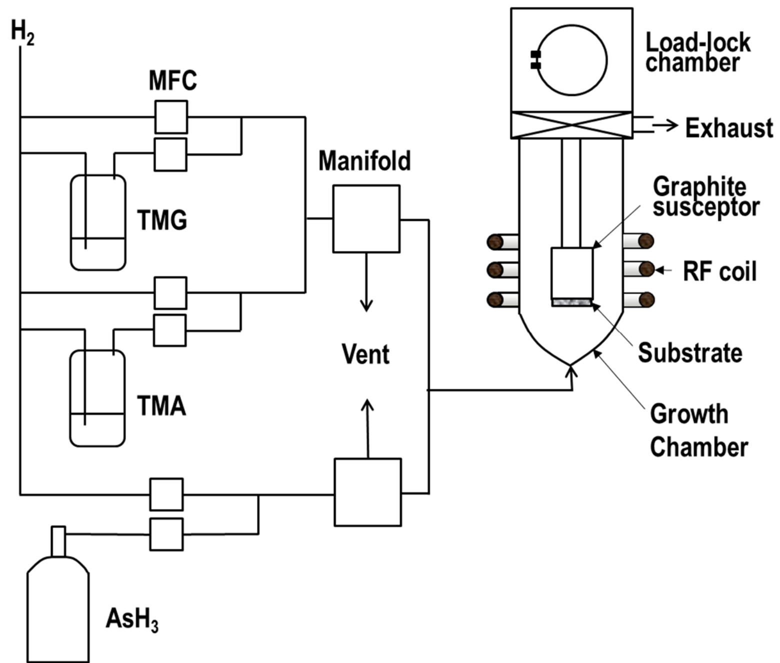

Fig. 2.

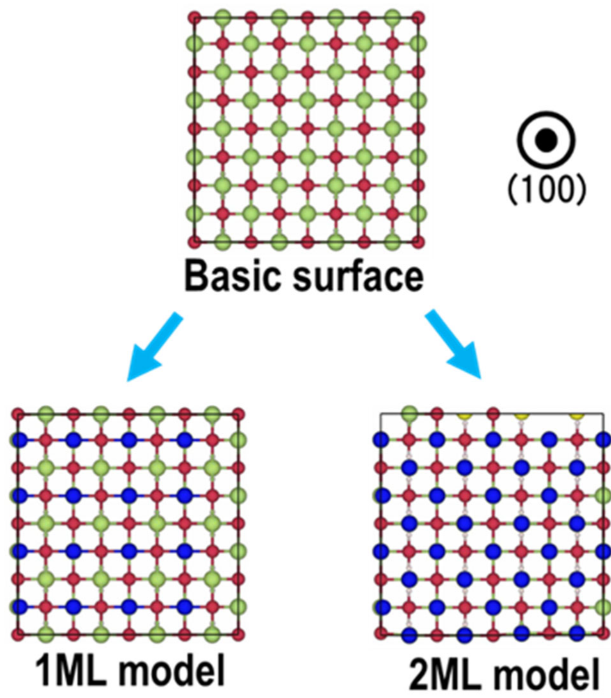

Fig. 3.

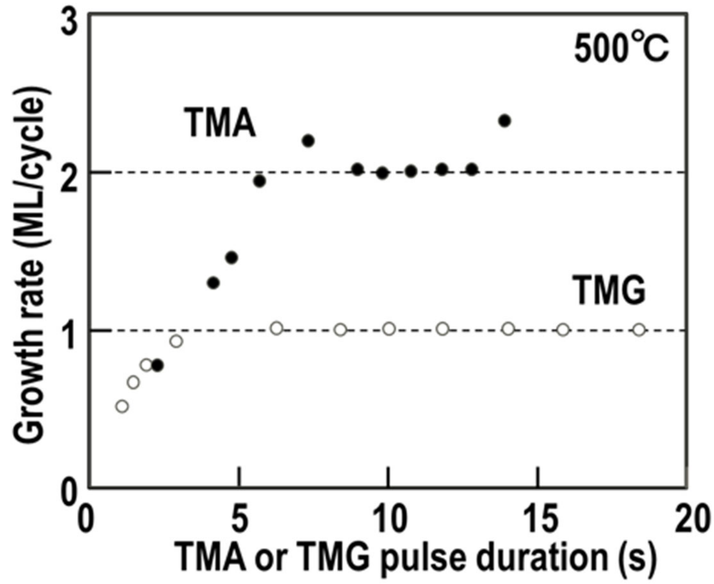

Fig. 4.

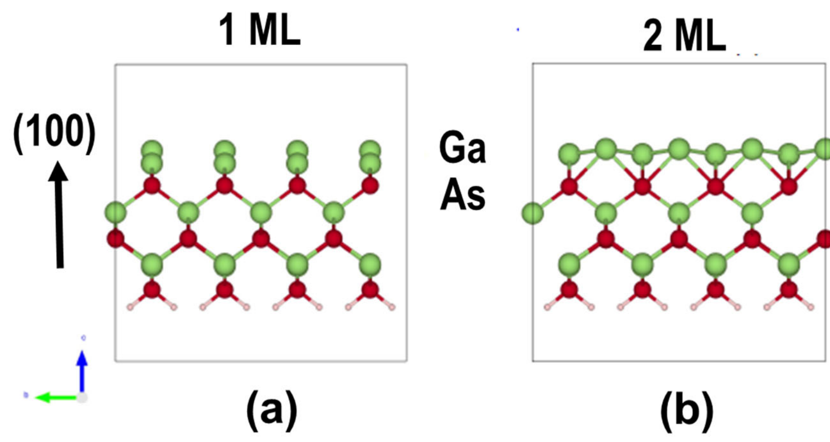

Fig. 5.

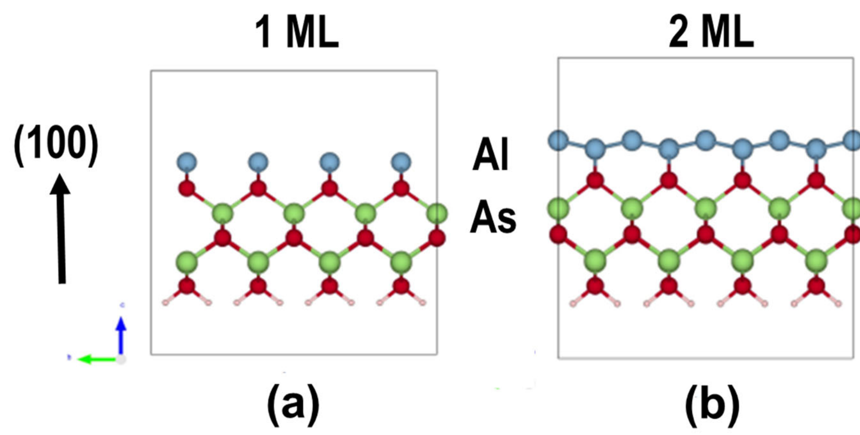

Fig. 6.

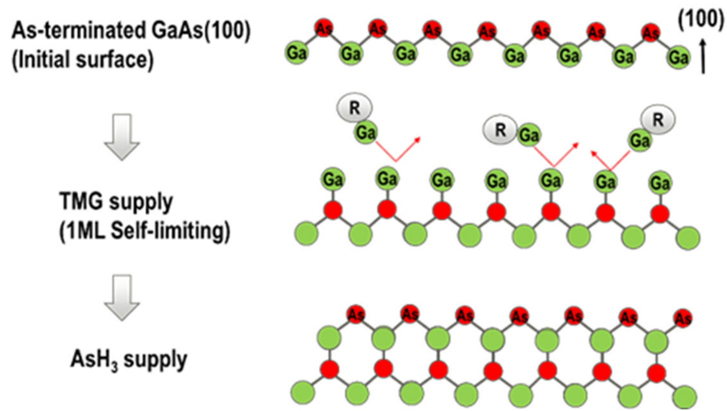

Fig. 7.

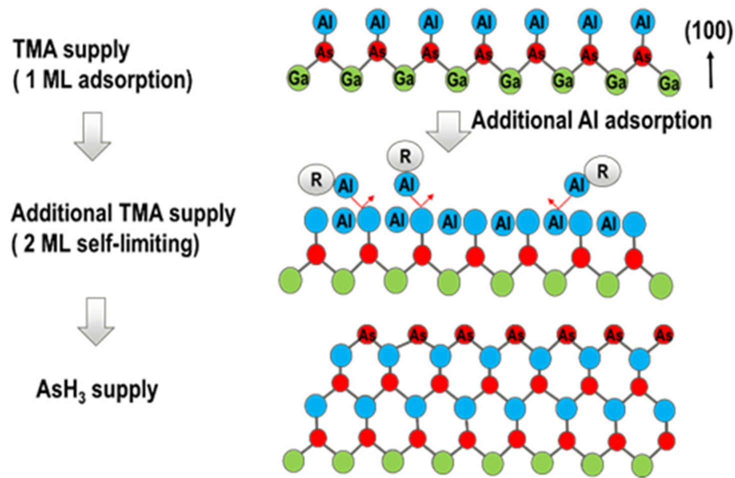

Fig. 8.